Optical Absorption Spectra of Coupled Nd^{3+} Ions in $NdCl_3$ and $NdBr_3$†

G. A. PRINZ
Department of Physics, The Johns Hopkins University, Baltimore, Maryland
(Received 31 May 1966)

The absorption spectra of single-crystal samples of pure $NdCl_3$ and $NdBr_3$ have been obtained at low temperatures (4.2 to 1.2°K) under high resolution in the region from 2700 Å to 1 μ for $NdCl_3$ and in the region 3000 to 7000 Å for $NdBr_3$. Aside from small shifts in the Stark multiplets of the order of 20 cm^{-1}, the principal difference from the spectrum of 1% $NdCl_3/LaCl_3$ is that each line is accompanied by two symmetrically placed satellites of comparable intensity, one on either side of the main line. Zeeman studies were made of the lines in fields up to 36 kOe, applied both parallel and perpendicular to the axis which joins the nearest-neighbor Nd^{3+} within the sample. The source of these additional lines is interactions coupling neighboring Nd^{3+} ions. Only a small part of this coupling is attributable to known, calculable interactions between the ions—electric dipole, magnetic dipole, and electric quadrupole. A satisfactory interpretation of the spectra can be obtained by assuming an additional coupling between Nd^{3+} neighbors i and j of the form $\mathcal{H}_{ij}=\mathcal{J}_{ij}S_{zi}S_{zj}$ where S_z is the z component of fictitious spin $\frac{1}{2}$. This coupling is assumed to be due to electron exchange. The sign and magnitude of the nearest-neighbor coupling has been obtained for the ground and five excited states in $NdCl_3$ and for the ground and five excited states in $NdBr_3$. The sign and magnitude of the next-nearest-neighbor coupling has been obtained for the ground and two excited states in $NdBr_3$.

INTRODUCTION

THE purpose of this paper is to expand the analysis of the experimental results reported[1] earlier for $NdCl_3$ and to present new results obtained from $NdBr_3$. Investigation of the optical absorption spectrum of concentrated rare-earth salts had been avoided because of the anticipated excessive line breadths and confusing satellite structure. It has been found, however, that with sufficiently thin crystals, low temperatures, and high resolution these problems can be overcome. The structure of the absorption lines and their Zeeman patterns in the pure salts is readily analyzed on the basis of the n-n (nearest-neighbor) and n-n-n (next-nearest-neighbor) coupling of Nd^{3+} ions.

I. EXPERIMENTAL RESULTS

The absorption spectra of single-crystal samples of pure $NdCl_3$ and $NdBr_3$ were obtained at low temperatures (4.2 to 1.2°K) under high resolution in the region from 2700 Å to 1μ for $NdCl_3$, and in the region 3000 to 7000 Å for $NdBr_3$. Zeeman studies were made of the lines in fields up to 36 kOe, applied both parallel and perpendicular to the n-n axis of the sample.

The techniques of obtaining absorption spectra at low temperatures are standard in this laboratory, and have been thoroughly described elsewhere.[2] Since the crystals are highly hygroscopic, they were encapsulated in fused quartz tubing with $\frac{1}{2}$ atm of He as an exchange gas. The temperatures quoted are the temperatures of the bath in which the encapsulated crystals were immersed, and when <4.2°K, they were determined from the vapor pressure above the bath as measured by a McLeod gauge.

The $NdCl_3$ spectra were recorded photographically on a 21-foot Paschen mounting using a 4-×7-in. grating having 1200 lines/mm. The $NdBr_3$ spectra were photographed on a 5-m, two-mirror Fastie spectrograph (Jarrell-Ash Model 72360). It incorporates a 10-in. plane grating having 300 lines/mm.

In the following discussion, since all the spectra were obtained at 4.2°K or lower, absorption is only observed from the lowest Stark level; hence, the "A_1 line" means the absorption line due to a transition from the ground state of the A_1 level.[3] As usual, polarization of the spectra refers to the direction of **E**, the electric vector of the incident radiation. In $NdCl_3$, σ polarization means ($\mathbf{E}\perp C_3$) and π is ($\mathbf{E}\|C_3$), where C_3 is both the optic axis of the hexagonal crystal, and the axis joining n-n Nd^{3+} ions. In $NdBr_3$, which is orthorhombic, we have adopted the convention of $\sigma(\mathbf{E}\|\hat{c})$ and $\pi(\mathbf{E}\|\hat{b})$, where $\hat{a}$, $\hat{b}$, $\hat{c}$ are the orthogonal unit vectors defining the crystallographic directions.[4] The reasons for this convention will be made clear later. All samples were

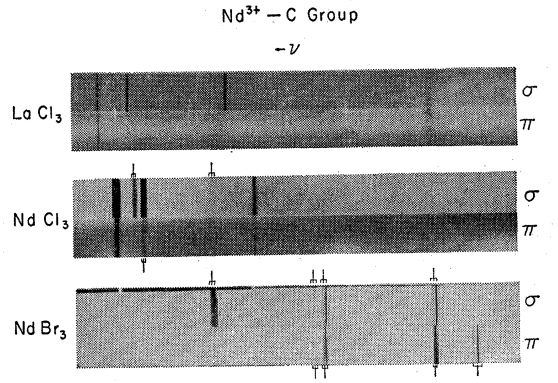

FIG. 1. C absorption group of Nd^{3+} ion in $LaCl_3$, $NdCl_3$, and $NdBr_3$. Region shown is 6260–6335 Å (180 cm^{-1}).

† This work supported in part by the U. S. Atomic Energy Commission.

[1] G. A. Prinz, Phys. Letters **20**, 323 (1966).

[2] G. H. Dieke and L. Heroux, Phys. Rev. **103**, 1227 (1956).

[3] For a complete listing of the Nd^{3+} levels see E. H. Carlson and G. H. Dieke, J. Chem. Phys. **34**, 1602 (1961).

[4] R. W. G. Wyckoff, *Crystal Structures* (Interscience Publishers, Inc., New York, 1964), 2nd ed., Vol. II.

≈0.1-mm thick, cut from single crystals grown in this laboratory by E. F. Williams.

Figure 1 shows the C absorption group of Nd^{3+} in three different crystals: $LaCl_3$, $NdCl_3$, and $NdBr_3$. Note that since the site symmetry in the two chlorides is the same (C_{3h}) the polarization is the same. The only changes are in the Stark splitting and in the appearance of a three-component structure for each line in $NdCl_3$ which was not overabsorbed. We shall refer to this structure as a triple, and observe that it must be due to interactions with the neighboring Nd^{3+} ions, since that is the only other physical change in environment in going from $LaCl_3$ to $NdCl_3$. The $NdBr_3$ spectra show even wider spaced triple structures and a significant alteration in the polarization and spacing of the Stark components. The former indicates even stronger interactions with neighboring Nd^{3+} ions, while the latter is caused by an alteration in the crystalline site symmetry.

The above observations were characteristic of all the observed absorption spectra.

Figure 2 shows the parallel Zeeman (Z_{II}) splitting of the $I_1(\pi)$ line in $NdBr_3$. In $NdCl_3$, Z_{II} means ($H\|C_3$) and $Z_\perp$ means ($H\perp C_3$). In $NdBr_3$ we adopt the convention of Z_{II} meaning ($H\|b$) and $Z_\perp$ is ($H\|c$). Note that the Z_{II} pattern separates into two sets of triples and the triple spacing is independent of field strength. In addition, each component of the triple sharpens to reveal that it is itself composed of several lines. The relative intensities within the pattern change with increasing field; the outer components of the triple fade, while the inner components are enhanced. The relative intensities of the fine-structure components within each triple component also are field-dependent. The maxima there shift to the outside of the pattern with increasing field. There is a five-component structure within each triple component, although due to the relative intensities not all are readily observed at a given field strength. Similar results were obtained for Z_{II} in $NdCl_3$, except that no sub-triple structure was resolved. For some lines, the shift in the relative intensities of the Zeeman components were opposite to the above behavior, but symmetric shifts were always observed. The sharpening effects of the parallel field often revealed structure not evident in the zero-field spectra.

Extensive Zeeman studies ascertained that the Zeeman splittings (in the absence of Paschen-Back effects from neighboring levels) were linear to within the limits of measurement, and that the triple spacings and sub-triple structure spacings were independent of field strength or temperature

The above observations are in sharp contrast to the $Z_\perp$ studies. In $NdCl_3$ there is a rapid broadening of the components of a triple, so that in high fields (36 kOe) the triple structure is obscured. The broad asymmetric lines which persist, appear to be blends of the former three components. There is also a breakdown in the

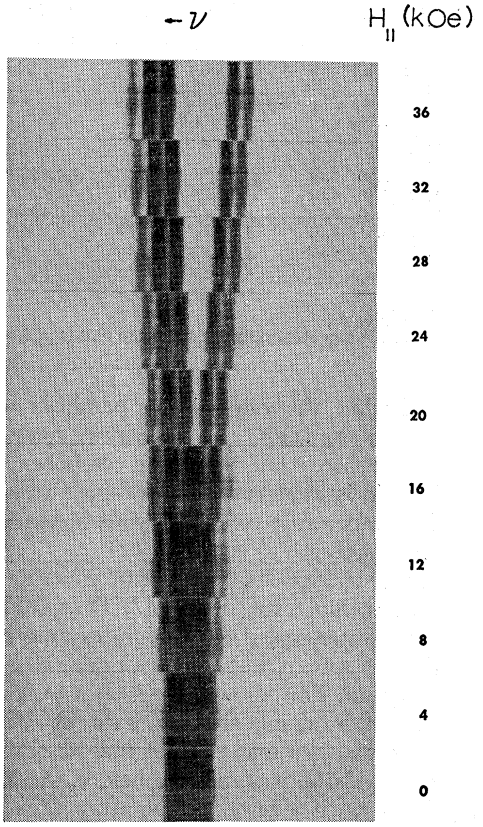

FIG. 2. Parallel Zeeman splitting of $I_1(\pi)$ in $NdBr_3$. Bath temperature is 1.5°K. Region shown is centered at $\lambda_{vac}=4241$ Å and is 5 Å (30 cm^{-1}) wide.

selection rules, allowing the strongest components of π to "leak through" on to σ, but the σ components do not appear in π. In $NdBr_3$ there is also a line broadening with increasing field, which, while sufficient to obscure any sub-triple structure, nevertheless allows the triple structure itself to persist in fields up to 36 kOe. There is also an apparent breakdown in the selection rules here, but the behavior is not clear cut. In some cases very weak π lines come through much stronger in σ, while strong σ lines do not appear in π. Other $Z_\perp$ patterns in $NdBr_3$ appear to be unpolarized.

Because of the above differences in the spectra and the amount of time needed to complete high-resolution Zeeman studies such as illustrated in Fig. 2, these initial investigations concentrated upon Z_{II} rather than $Z_\perp$.

A. Temperature Effects

At "high" temperatures (4.2°K in most cases) the relative intensities of the three members of any given triple were approximately 1:2:1. By lowering the temperature of the sample, the longer wavelength member became less intense, while the other two were enhanced and all members exhibited a sharpening. The relative intensities of the lines in a Zeeman pattern could be similarly affected. If the temperature of the crystal

TABLE I. Comparison of splitting factors (in Lorentz units).

Level	$LaCl_3$[a] $s_\parallel$	$s_\perp$	$s_\parallel(Z_1)$	$NdCl_3$ $s_\parallel$	$s_\perp$	$s_\parallel(Z_1)$	$NdBr_3$ $s_\parallel$	$s_\perp$	$s_\parallel(Z_1)$
Z_1[b]	−4.00	1.76		−4.4	1.56		−3.8	[c]	
B_2	8.47			8.17		4.23			
B_4	1.33		4.01	1.35		4.41			
C_3	−9.10	0.10	3.98				−7.85		3.80
G_1	1.19	4.40	4.01	1.15		4.40			
I_1	0.59	0.60	3.98				0.45	[c]	3.70
I_2	1.17	3.41	4.01	1.34		4.29			
K_1	1.07	2.14	4.02	1.06	2.15	4.48			

[a] From Carlson.
[b] Weighted mean value.
[c] Assignment of the two obtained values 0.70 and 0.02 is undetermined.

was lowered while the value of the parallel magnetic field was held constant, the outermost components became less intense, while the inside components were enhanced. This is analogous to the effect caused by holding the temperature constant, while increasing the magnetic field strength as shown in Fig. 2.

Temperature changes had a dramatic effect upon the Zeeman pattern illustrated in Fig. 2. That study was made using a water-cooled AH-6 high-pressure Hg arc as a continuous source, but with a Corning 0160 filter before the crystal. This allowed $\lambda > 3000$ Å to fall upon the crystal. Maintaining the He bath at 1.5°K, a similar study was then made except that an additional filter (BL-430-43-H) was placed before the crystal allowing it to reach a lower temperature. This interference filter was centered at the absorption line ($\approx$4300 Å) and had a pass-band half-width of 200 Å. Only one of the five components within each triple component remained prominent at the lower temperature. These were the same components which tended toward survival at high fields.

Although all the lines of the $NdCl_3$ and $NdBr_3$ spectra which were not overabsorbed showed the triple structure, only σ, π lines proved to be suitable for analysis. In $NdCl_3$, this meant transitions only to upper levels having crystal quantum number $\mu=\frac{1}{2}$. The Zeeman splitting factors for the observed levels are given in Table I. Comparison of the splitting factors in pure $NdCl_3$ and 1% $NdCl_3$ shows that to within the limits of measurement, except for the Z_1 level, they are changed little or not at all. This is reasonable, since they are all $\mu=\frac{1}{2}$ levels with $J<11/2$, except for Z_1, which is $\mu=\frac{5}{2}$, a mixture of $M_J=\frac{5}{2}$ and $M_J=\frac{7}{2}$. The sharper lines of 1% $NdCl_3$ enabled the splitting factors to be determined with greater precision. This was especially true for $s_\perp$, so except for $s_\perp(Z_1)$ we shall use the 1% values for calculations. Since $s_\parallel(Z_1)$ could be determined separately from each $\mu=\frac{1}{2}$ line's Zeeman pattern, the uncertainty in its value is based on the variation in these determinations rather than just the estimated accuracy of measurement. $s_\perp(Z_1)$ was then calculated from $s_\parallel(Z_1)$. It was found to be consistent with the value obtained from the $Z_\perp$ splitting of K_1 and considered to be more reliable.

II. ANALYSIS

A. Crystal Structure

$NdCl_3$ has the same well-known crystal structure as hexagonal $LaCl_3$, while $NdBr_3$ is layered orthorombic.[4] Of immediate interest, however, are only the n-n and n-n-n relationships of Nd^{3+} ions, and in this respect the geometries of the two structures retain certain similarities. In $NdCl_3$ the n-n are located along chains parallel to the C_3, or optic axis, of the crystal. Each Nd^{3+} ion has, therefore, two n-n, one located above it and one below it along the chain. The same situation exists in $NdBr_3$, except that the chains here are parallel to the b axis of the unit cell, which is not an optic axis. In both cases, the n-n-n are on neighboring parallel chains, and the chains are staggered so that a Nd^{3+} ion on one chain is displaced along the chain axis to be midway between two Nd^{3+} ions on the neighboring chains. Hence, a given Nd^{3+} ion has two n-n-n on each neighboring chain. The principal difference between the two structures is that in $NdCl_3$ there are three chains immediately neighboring a given chain, while in $NdBr_3$ there are two. In $NdCl_3$ these three neighboring chains form an equilateral triangular array, giving rise to the hexagonal crystal structure; while in $NdBr_3$, a chain is coplanar with its two neighboring chains, and these planes form the basis of the layered orthorhombic structure. In summation, then, in $NdCl_3$ each Nd^{3+} ion has two n-n and six n-n-n: while in $NdBr_3$ each Nd^{3+} ion has two n-n and four n-n-n. The distances between Nd^{3+} ions are[4]:

$$NdCl_3: r_{n\text{-}n}=4.231 \text{ Å}, \quad r_{n\text{-}n\text{-}n}=4.758 \text{ Å},$$
$$NdBr_3: r_{n\text{-}n}=4.11 \text{ Å} \quad r_{n\text{-}n\text{-}n}=5.02 \text{ Å}.$$

The layered structure of $NdBr_3$ caused it to cleave very readily parallel to these layers, i.e., parallel to the c-b plane. Since only very thin cleavage sections were suitable for this study, all spectra were taken using the above type of cleavage section. All the measurements were therefore made with the light traveling parallel to $\hat{a}$, and because of the similarity to $NdCl_3$, $\hat{b}$ was treated as the $\hat{z}$ direction. This formed the basis for the conventions adopted concerning σ, π, $Z_\parallel$, and $Z_\perp$ discussed earlier. For $NdBr_3$, $Z_\perp$ and $s_\perp$ are actually Z_x and s_x, and unlike $NdCl_3$, in general $s_x \neq s_y$.

B. Coupling Mechanisms

We consider the coupling Hamiltonian between Nd^{3+} ions i and j in $NdCl_3$

$$\mathcal{H}_{ij}=A_{ij}S_{zi}S_{zj}+B_{ij}(S_{+i}S_{-j}+S_{-i}S_{+j}), \qquad (1)$$

where S_{zi} is the z component of the fictitious spin of the ith ion, $S_{+i}=S_{xi}+S_{yi}$, etc. Since all of the Stark levels of Nd^{3+} are Kramers doublets, we have a fictitious spin $\frac{1}{2}$.

Electric dipole (ED). For an ion in the ground state, which has the crystal quantum number $\mu=\frac{5}{2}$, the static

ED moment is zero. Since we shall not be considering the cases of more than one ion not in the ground state, we shall not have static ED coupling between ions.

Electric quadrupole (*EQ*). As discussed by Baker for Nd^{3+} in LaES,[5] the first-order perturbation due to EQ moments coupling two neighboring ions merely shifts, but does not split the Stark levels. He shows, however, that a second-order perturbation involving higher levels does cause a coupling which can be put in the form of Eq. (1). We shall adopt his calculation to obtain an estimate for $NdCl_3$.

Magnetic dipole (*MD*). Coupling the ions through their MD moments yields (choosing z along the n-n axis)

$$A_{ij}=(1-3\cos^2\theta_{ij})\beta^2 s_{11i}S_{11j}/r_{ij}^3, \tag{2a}$$

$$B_{ij}=\beta^2 s_{1i}s_{1j}/r_{ij}^3, \tag{2b}$$

where $\cos\theta_{ij}=1$ for n-n. (β=Bohr magneton.)

For n-n-n we have additional terms in the Hamiltonian of the form $S_{+i}S_{+j}$, $S_{+i}S_{zj}$, etc. As we shall see in the discussion of the $S_{+i}S_{-j}$ terms, the additional MD terms are probably negligible when discussing the principal features of the optical spectrum.

Exchange (*Ex*). If we consider an anisotropic exchange coupling of the form

$$\mathcal{H}_{ij}(\mathrm{Ex})=\mathcal{J}_{ij}(z)\mathfrak{S}_{zi}\mathfrak{S}_{zj}+\mathcal{J}_{ij}(x,y)(\mathfrak{S}_{xi}\mathfrak{S}_{xj}+\mathfrak{S}_{yi}\mathfrak{S}_{yj}) \tag{3}$$

between the total real spins of the ions $\mathfrak{S}$, when written in terms of fictitious spin S, we have in Eq. (1)

$$A_{ij}=(g_ig_j)^{-1}(g_i-1)(g_j-1)s_{11i}s_{11j}\mathcal{J}_{ij}(z) \tag{4a}$$

$$B_{ij}=(g_ig_j)^{-1}(g_i-1)(g_j-1)s_{1i}s_{1j}\mathcal{J}_{ij}(x,y). \tag{4b}$$

For isotropic exchange, $\mathcal{J}_{ij}(z)=\mathcal{J}_{ij}(x,y)$.

In $NdBr_3$ since we do not have an uniaxial crystal, Eq. (1) should be written as

$$\begin{aligned}\mathcal{H}_{ij}&=a_{ij}S_{zi}S_{zj}+b_{ij}S_{xi}S_{xj}+c_{ij}S_{yi}S_{yj}\\&=a_{ij}S_{zi}S_{zj}+\tfrac{1}{4}(b_{ij}+c_{ij})(S_{+i}S_{-j}+S_{-i}S_{+j})\\&\quad+\tfrac{1}{4}(b_{ij}-c_{ij})(S_{+i}S_{+j}+S_{-i}S_{-j}).\end{aligned} \tag{5}$$

For MD, $a_{ij}=A_{ij}$ as defined by Eq. (2a), but $b_{ij}=\beta^2 s_{xi}s_{xj}(r_{ij})^{-3}$ and $c_{ij}=\beta^2 s_{yi}s_{yj}(r_{ij})^{-3}$. There is as yet insufficient data to determine b_{ij} and c_{ij}. Only the MD $S_{zi}S_{zj}$ contributions have been calculated for $NdBr_3$.

Similarly, for exchange in $NdBr_3$, (4b) must be corrected by the replacement

$$s_{11i}s_{11j}\mathcal{J}_{ij}(x,y)\rightarrow s_{xi}s_{xj}\mathcal{J}_{ij}(x)+s_{yi}s_{yj}\mathcal{J}_{ij}(y).$$

C. $S_{zi}S_{zj}$ Coupling

If we consider only $S_{zi}S_{zj}$ n-n coupling, the S_{zi} are good quantum numbers and we can have states where all of the S_{zi} are specified. This means that a state can be specified in terms of the orientations of the magnetic moments of the individual ions. In a given state, therefore, the neighborhood (i.e., the orientation of the moments of neighboring ions) of any given ion can be specified exactly. Furthermore, the radiation operators are single-particle operators, which cause transitions between levels of the system in which only one ion at a time is excited. These conditions allow us to adopt the point of view of considering the neighborhood of a given ion to remain constant, while the ion undergoes a transition to an excited Stark level and possibly "flips" its magnetic moment. The energy difference of the transition will then depend only upon the neighborhood and the Stark levels involved.

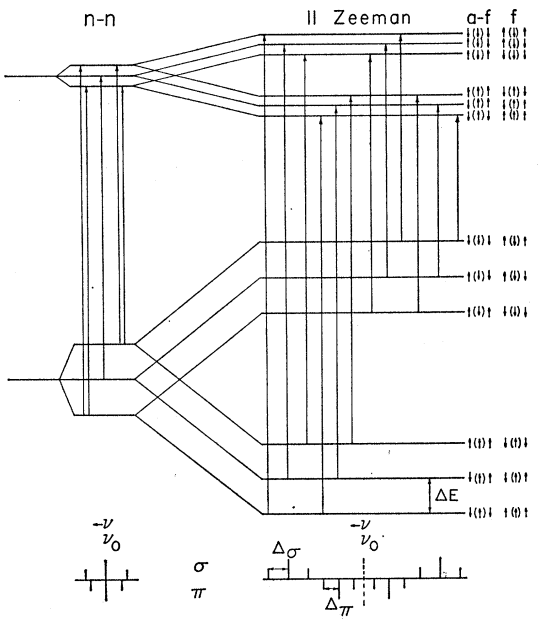

FIG. 3. Pseudo-energy-level diagram (energy difference diagram) showing origin of triples for either ferromagnetic (f) or antiferromagnetic (af) n-n $S_{zi}S_{zj}$ coupling and parallel Zeeman effect.

On this basis, one can construct a diagram which illustrates the energy differences involved in the several possible transitions associated with a given electronic transition. This diagram, Fig. 3, resembles the resulting energy-level diagram one would obtain if the interactions with n-n were considered to be a perturbation of the single ion levels, splitting each Stark level into a n-n manifold. The labels on the levels describe the neighborhood. Here (↓) or (↑) represent the magnetic moment of the ion in question and ↓ or ↑ represent that of the two n-n, above and below, along the z axis. There are two alternate sets of labels on the levels. One assumes antiferromagnetic coupling between n-n (af), and the other assumes ferromagnetic coupling (f).

Note that this energy-level scheme groups together quite different nondegenerate states of the crystal into one level. The important point is that degenerate transitions have been grouped together. For this reason one must be careful when drawing conclusions from this energy difference diagram about additional perturbations of the system.

[5] J. M. Baker, Phys. Rev. 136, A1341 (1964).

The electric dipole selection rules for an odd-electron atom in C_{3h} symmetry ($NdCl_3$) are $(\sigma)\Delta\mu=\pm 4$, and $(\pi)\Delta\mu=\pm 3$. A consequence of these rules, and of the fact the ground-state splitting factor $s_{II}(Z_1)$ is negative, is that a σ transition corresponds to a flipping of the magnetic moment during a transition, if the upper state splitting factor s_{II}' is positive. If s_{II}' is negative, then a π transition corresponds to a moment flip.

Whether the σ or π triple is wider spaced depends upon *both* the sign of s_{II}' and the sign of A_{ij}'. In Fig. 3, $s_{II}'>0$ and the upper-state coupling A_{ij}' is of the same sign as the ground-state coupling A_{ij}. If just A_{ij}' changes sign, then the Δ_σ and Δ_π labels in Fig. 3 should be reversed. If s_{II}' changes sign, every σ, π label is interchanged. Since the n-n splitting is given by $\Delta E=\frac{1}{2}A_{ij}$, from Fig. 3 we have

$$\Delta_\sigma=\tfrac{1}{2}A_{ij}+\tfrac{1}{2}A_{ij}', \quad A_{ij}=\Delta_\sigma+\Delta_\pi,$$
$$\Delta_\pi=\tfrac{1}{2}A_{ij}-\tfrac{1}{2}A_{ij}', \quad A_{ij}'=\Delta_\sigma-\Delta_\pi.$$

Parallel Zeeman Effect. An externally applied magnetic field along the n-n axis will maintain the z axis of quantization, but it will remove a twofold degeneracy which existed in each of the transitions. For example, in the absence of a parallel magnetic field, the two transitions of Fig. 3, $\uparrow(\uparrow)\uparrow \rightarrow \uparrow(\uparrow)'\uparrow$ and $\downarrow(\downarrow)\downarrow \rightarrow \downarrow(\downarrow)\downarrow'$, where $(\ )'$ denotes the upper state, represented equal energy differences. If the upper-state splitting factor (or, equivalently, its magnetic moment) differs from that of the ground state, these two transitions will differ in energy by an amount proportional to the magnetic field strength. This result can be nicely demonstrated using the energy difference diagram of Fig. 3. The parallel Zeeman effect on the observed transitions can be reproduced by a symmetric splitting of the n-n levels proportional to s_{II} for that level.

The field will cause alignment of magnetic dipole moments, and the population of sites in a neighborhood aligned with the field will increase at the expense of the population of sites in anti-aligned neighborhoods. This will have the effect of changing the relative intensities of the lines within a triple. At high temperatures in the absence of a magnetic field the ratio of the intensities is about 1:2:1. In a strong magnetic field, however, only the transitions arising from ions in neighborhoods which are largely aligned with the field will persist. Ultimately, in a field large enough to saturate the crystal sample, only completely aligned neighborhoods could exist, and only one sharp line would persist in the spectrum.

From Fig. 3 we can see that the spectra would be affected in the following manner. The sets of triples will separate symmetrically in both σ and π. Assuming $\Delta E'<\Delta E(Z_1)$ and $0<s_{II}'<|s_{II}(Z_1)|$, the outer components of the Zeeman components would fade, while the inside components would be enhanced as the strength of the field increased. Each member of the shorter wavelength triple would get stronger than its corresponding member in the longer wavelength triple. Ultimately the only remaining line would be the long-wavelength member of the short-wavelength triple. This description fits the observed spectra and depends crucially upon the choice of antiferromagnetic n-n ground-state coupling. Neither choice of coupling for the excited state will correctly predict the observed intensity behaviors if the ground-state coupling is assumed to be ferromagnetic. Although there were other behaviors observed for the intensities within a Zeeman pattern, they could in every case be understood on the basis of a change in s_{II}' or ferromagnetic A_{II}'.

Only a slight extension of the above remarks is necessary to cover n-n-n $S_{zi}S_{zj}$ coupling. In addition to the two n-n we now have six ($NdCl_3$) or four ($NdBr_3$) n-n-n whose orientations must also be specified in order to describe a neighborhood. All of the former remarks concerning transitions still hold, hence we can also represent the n-n-n effects on a pseudo energy-level diagram. This is done in Fig. 4 for $NdCl_3$. Here each level from a n-n manifold is shown to be further split into a n-n-n manifold. In the n-n-n manifolds the orientations of the magnetic moments of the six n-n-n are represented by (+) or (−). The levels as labeled assume ferromagnetic n-n-n coupling. The same "selection rules" are employed as previously, to yield the transitions shown. The relative strengths of the transitions reflect only the degeneracy of each n-n-n level, and represent, therefore, a high-temperature approximation. The degeneracy of each n-n-n level is merely the number of ways the neighborhood of six n-n-n can be chosen and still satisfy the labeling of that level. These degeneracies are

Neighborhood	Degeneracy
6(+)0(−)/0(+)6(−)	1
5(+)1(−)/1(+)5(−)	6
4(+)2(−)/2(+)4(−)	15
3(+)3(−)	20

When all of the n-n levels are considered, we arrive at a total spectral pattern for the transitions from the ground Stark level to an excited Stark level as shown at the bottom of Fig. 4. The transitions will yield resolved n-n-n multiplets only if the lines are sufficiently sharp, otherwise one broad line will be observed for each transition from one n-n level to another, as indicated by the dashed envelope. Because of the different width of the n-n-n multiplets in the two cases and the resulting overlap of lines, the triple will in general be much better resolved in one polarization than in the other.

The effect of a magnetic field applied along the z axis upon the n-n-n manifold can be represented as it was in Fig. 3 for the n-n manifold. As before, we observe that the field will cause alignment of magnetic dipole moments, and the population of sites in a neighborhood aligned with the field will increase at the expense of the

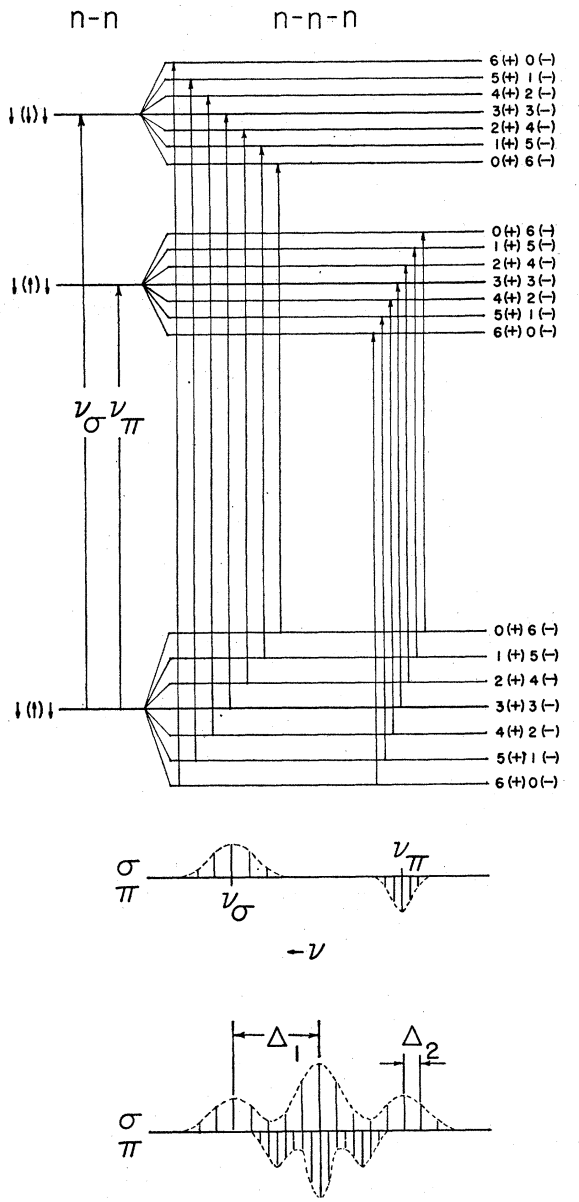

FIG. 4. Transitions between levels of n-n-n manifolds showing origin of broadening or additional structure within each component of a triple due to n-n-n $S_{zi}S_{zj}$ coupling.

population of sites in anti-aligned neighborhoods. The lines will sharpen, because the population distributed over the seven levels of a n-n-n manifold will gradually concentrate, with increasing field strength, into the level corresponding to the six n-n-n being aligned with the field. This will tend to eliminate the broadening discussed earlier caused by the unresolved fine structure from the n-n-n manifolds. This sharpening is accompanied by a shift in the peak of the population distribution from the center to the edge of the n-n-n manifold. Since the peaks in all the manifolds shift uniformly, the mutual separation of the n-n levels is unaffected, but we can expect the Zeeman splitting to be altered. The Zeeman splitting may not be linear until sufficiently high fields are reached. This is most likely to occur in lines which were quite broad in zero field and least likely in those which were sharp. Whether the splitting factor will be increased or diminished depends upon the sign of the n-n-n coupling for that level. Of course for $NdBr_3$, there should be only five n-n-n components within a n-n component of a triple, since there are only five levels within a n-n-n manifold.

From Fig. 4 we have for the n-n-n structure $\Delta E_2 = \frac{1}{2}\{\Delta_2(\sigma)+\Delta_2(\pi)\}$ and $\Delta E_2' = \frac{1}{2}\{\Delta_2(\sigma)-\Delta_2(\pi)\}$, where $\Delta E_2 = \frac{1}{2}A_{ij}$(n-n-n) is the separation between the levels of the n-n-n manifold.

D. $(S_{+i}S_{-j}+S_{-i}S_{+j})$ Coupling

Svare and Seidel {SS}[6] have suggested a simple method to estimate the effects of the S_+S_- terms upon the EPR spectra of neodymium ethylsulfate (NdES), and obtain good agreement with experiment. Their method is applied here to the optical spectra couched in the terms of this discussion.

The lowest order effect of the $S_{+i}S_{-j}$ terms will be to remove the degeneracy and separate those states which are both degenerate with respect to $S_{zi}S_{zj}$ and coupled by $S_{+i}S_{-j}$.

If one considers only S_+S_- coupling with one n-n, as pointed out by {SS} one must then consider the orientation of the two ions above and below the two in question. For example, consider the following two transitions in which one of the ions, indicated by the parentheses, in a string of four neighboring ions undergoes electronic excitation to a state indicated by a prime: $\uparrow(\uparrow)\downarrow\uparrow \rightarrow \uparrow(\uparrow)'\downarrow\uparrow$ and $\uparrow\downarrow(\uparrow)\uparrow \rightarrow \uparrow\downarrow(\uparrow)'\uparrow$. These two transitions are equivalent to the following transition in terms of the labels used in Fig. 3: $\uparrow(\uparrow)\downarrow \rightarrow \uparrow(\uparrow)'\downarrow$. The two lower states are degenerate with respect to $S_{zi}S_{zj}$, and they are coupled by $(S_{+i}S_{-j}+S_{-j}S_{+j})$. Note that the excited states are not so coupled. The effect of S_+S_- is to split each of the twofold degenerate lower states into a symmetric and antisymmetric pair, e.g.,

$$|s\rangle = (\sqrt{\tfrac{1}{2}})\{|\uparrow\uparrow\downarrow\uparrow\rangle + |\uparrow\downarrow\uparrow\uparrow\rangle\},$$
$$|a\rangle = (\sqrt{\tfrac{1}{2}})\{|\uparrow\uparrow\downarrow\uparrow\rangle - |\uparrow\downarrow\uparrow\uparrow\rangle\}.$$

The upper state which remains twofold degenerate could also be described by a symmetric and antisymmetric pair. Since the radiation operator is symmetric under interchange of particles, only states of the same symmetry will be joined by a transition. As a result, the previously twofold degenerate transition will be symmetrically split by the S_+S_- coupling into two distinguishable absorption lines. What is observed experimentally, of course, is a superposition of the split line from S_+S_- coupled sites upon the unsplit line from uncoupled sites. The S_+S_- coupling will therefore manifest itself as a symmetric broadening of the affected lines.

[6] I. Svare and G. Seidel, Phys. Rev. 134, A172 (1964).

This broadening will be proportional to the probability of S_+S_- coupled sites, and the coefficient B_{ij}.

This broadening will only effect states involving all ions in the lowest Stark level, since there are no arrangements, given one ion in an excited electronic state, which will be both $S_{zi}S_{zj}$ degenerate and coupled by S_+S_-. In fact, upon consideration, one can show that only two components of a triple will be broadened. The levels labeled $\uparrow(\uparrow)\uparrow$ and $\downarrow(\downarrow)\downarrow$ of Fig. 3 are unaffected. Hence, we obtain the result that, considering S_+S_- coupling to one n-n, we should observe the same amount of broadening of two components of each triple throughout the spectrum.

A similar estimate can be made for S_+S_- coupling between n-n-n. Here we must consider six particles, the n-n-n pair and each of their n-n. The n-n-n coupled by S_+S_- will only be those which have similar orientations of n-n. Every transition in each polarization will be affected, but again it is only because of splittings in lower state levels, not in excited states, because given one ion in an excited electronic state, those states which are degenerate are not coupled by S_+S_-, and those which are coupled are not degenerate.

The lower states can be formed into a symmetric and antisymmetric pair, splitting the lower state and broadening the observed absorption line as discussed earlier for n-n coupling. The only change is now in the magnitude of the splitting (B_{ij}) and the probability of the site.

Application of a magnetic field, along the x direction, introduces into the Hamiltonian the term

$$H_i(\perp) = -\beta H s_\perp \tfrac{1}{2}(S_{+i}+S_{-j}).$$

For the $\mu=\frac{1}{2}$, $\mu=\frac{5}{2}$ states we shall be interested in, $s_\perp \neq 0$ in first order, and the effect of a perpendicular magnetic field applied to the crystal is again to cause each level of the n-n manifold of Fig. 3 to split, but this time with a splitting factor $s_\perp$. It mixes each state with its Kramers conjugate state, which tends to break down the polarization selection rules based upon μ as a good quantum number. In addition, it will mix neighborhoods in a manner not amenable to our former analysis. since S_+ or S_- alone, unlike S_+S_-, will flip only one spin at a time. The effect of this mixing will be to break down the selection rules based upon constancy of neighborhoods which created the symmetric triple pattern.

E. Calculations

Electric quadrupole (*EQ*). Two changes must be made in Baker's calculation to obtain an estimate for the splitting of the ground state in $NdCl_3$ due to n-n EQ-EQ interaction. First the coefficient $A = 3e^2\langle r^2\rangle^2 \times \langle J\|\alpha\|J\rangle^2/8\epsilon R^5 hc$ is recalculated using $\langle r^2\rangle = 1.001 a_0^2$ (mean-square radius of the $4f$ electrons)[7] and $R = 4.231$ Å (interionic distance). ϵ is an effective dielectric constant. We obtain $A = (1/\epsilon)(1.04\times 10^{-4}\ \text{cm}^{-1})$.

The second change is in the sum of second-order perturbation theory matrix elements. Since the composition of the states within the lowest Stark manifold are not greatly changed going from lanthanum ethylsulfate (LaES) to $NdCl_3$, an order-of-magnitude estimate can be obtained by merely correcting the energy differences (E_i-E_j) appearing in the denominator of the summation. It is a good approximation that the energy levels are unformly compressed by $\approx 20\%$, so we can say

$$(E_i-E_j)_{NdCl_3} = (0.8)(E_i-E_j)_{LaES}.$$

We then obtain for an estimate

$$A_{ij} = (1/\epsilon)^2(0.06\times 10^{-4}\ \text{cm}^{-1}),$$
$$B_{ij} = -(1/\epsilon)^2(0.33\times 10^{-4}\ \text{cm}^{-1}).$$

Since $\epsilon \geq 1$, it is apparent from the observed splittings in Table II that EQ coupling makes a negligible contribution for both ions in the ground state. No estimate was made for one ion in an excited state, and because of the rapid increase of R^5, n-n-n contributions to the ground-state splitting would be negligible.

Magnetic dipole (*MD*). $\frac{1}{2}A_{ij}$(MD) is just ΔE(MD) given in Table II for each level. B_{ij} is the upper limit for our estimate of S_+S_- broadening. Since to first order this broadening affects only the ground state, we need only consider $s_\perp(Z_1)$. For n-n in $NdCl_3$, $B_{ij}(Z_1) = 0.01$ cm^{-1}.

Exchange (*EX*). The residue of the splittings ΔE are attributed to exchange in Table II. The determination of the sign (i.e., af or f) of the exchange coupling depends upon the behavior of the intensities in the parallel Zeeman patterns. Thus the amount of splitting ΔE attributed to exchange may be greater or less than the observed splitting of a level, depending upon the total magnetic character assigned to that level and the amount of calculated dipolar splitting. The dipolar splitting is ferromagnetic for n-n and antiferromagnetic for n-n-n. From Eq. (4a), the g factors and splitting factors are divided out and the values of the exchange integrals themselves $\mathcal{J}(z)_{ij}$ are given in Table III.

If we assume isotropic exchange $\{\mathcal{J}(x,y) = \mathcal{J}(z)\}$, from Eq. (4b) we obtain for n-n in $NdCl_3$

$$B_{\text{n-n}}(Z_1) = 0.10\ \text{cm}^{-1}.$$

In a recent paper, Eisenstein, Hudson, and Mangum concluded $\mathcal{J}(\text{n-n}) = -3\mathcal{J}(\text{n-n-n})$ in $NdCl_3$, which implies for n-n-n

$$B_{\text{n-n-n}}(Z_1) = 0.03\ \text{cm}^{-1}.$$

While the latter broadening is small, the former is of sufficient size to obscure the n-n-n structure in the $NdCl_3$ spectra.

No estimates can be made of $B_{ij}(Z_1)$ in $NdBr_3$ until $s_x(Z_1)$ and $s_y(Z_1)$ have been determined.

[7] We use here the estimate given by A. J. Freeman and R. E. Watson, Phys. Rev. **127**, 2058 (1962). Baker's calculation uses $(1/\epsilon)\langle r^2\rangle^2 = 0.78$ Å^4 (Ce^{3+} in cerium ethylsulfate) and $\langle r^2\rangle_{Nd}/\langle r^2\rangle_{Ce} = 1.5$. The latter appears incorrect, and the former does not agree with Freeman and Watson for $\epsilon \geq 1$.

TABLE II. Splittings of energy levels (ΔE) and spectral lines ($\Delta_{\sigma,\pi}$) (in units of cm^{-1}).

Level	Observed Δ_σ	Observed Δ_π	Observed ΔE	$\Delta E(Z_1)$	Magnetic dipole (ferro) ΔE	Non-dipolar ΔE coupling	
			$NdCl_3$(n-n)				
Z_1[a]			0.70±0.03		0.11	0.81	af
B_2	0.96±0.07	0.33±0.08	0.32±0.08	0.65±0.08	0.21	0.53	af
B_4	0.52±0.02	0.88±0.02	0.18±0.02	0.70±0.02	0.04	0.14	f
G_1	0.71±0.04	0.76±0.02	0.02±0.02	0.73±0.03	0.03	0.01	af
I_2	0.74±0.01	0.62±0.02	0.06±0.02	0.68±0.02	0.04	0.10	af
K_1	0.88±0.02	0.55±0.05	0.33±0.04	0.72±0.04	0.03	0.36	af
			$NdBr_3$(n-n)				
Z_1[a]				1.02±0.02	0.09	1.11	af
B_1	1.01±0.05	1.07±0.06	0.03±0.06	1.04±0.06			af
B_2	0.98±0.10	1.05±0.03	0.04±0.10	1.01±0.10			af
C_2	1.28±0.01	0.71±0.02	0.29±0.02	1.00±0.02	0.18	0.11	f
C_3	1.08±0.02	0.95±0.03	0.07±0.03	1.01±0.03			af
I_1	1.09±0.03	0.96±0.02	0.07±0.03	1.03±0.03	0.01	0.08	af
			$NdBr_3$(n-n-n)				
Z_1[a]				0.20±0.01	0.01	0.21	f
C_2	0.26±0.01	0.12±0.01	0.07±0.01	0.19±0.01	0.00	0.07	af
I_1	0.19±0.01	0.22±0.01	0.02±0.01	0.20±0.01	0.02	0.00	...

[a] Weighted mean value.

III. CONCLUSION

The appearance of the additional structure within each line of the absorption spectra of $NdCl_3$ and $NdBr_3$ can be readily analyzed on the basis of just $S_{zi}S_{zj}$ interactions between n-n and n-n-n. The pseudo-energy-level diagram based upon the idea of the ion's neighborhood remaining fixed while the ion undergoes a transition proved to be consistently successful, not only in explaining the early observations on $NdCl_3$. but in predicting the results from $NdBr_3$. Only part of the splittings appear to be attributable to calculable interactions, principally coupling between magnetic dipole moments. If the remainder of the splittings are due to exchange coupling, it undergoes wide variation from level to level. High-resolution spectroscopic studies such as these provide information about couplings between ions not only for the ground state, but for the excited states as well. Although ground-state information can also be obtained via EPR studies, often the resonance lines in concentrated salts are too broad to yield useful information. More important, however is that it appears a systematic study can be made of the dependence of the exchange coupling in an insulator upon the wave fuuctions, since the vast amount of work done on the trichlorides makes them among the best understood of the paramagnetic crystals.

The apparent "Ising" nature of the coupling has induced Marsh to apply Ising statistics to $NdCl_3$ with reasonable success.[8] It may be that the environmental anisotropy reflected in $s_{\parallel}(Z_1)/s_{\perp}(Z_1)$ is sufficient to account for the Ising behavior. If this is so, the increased sharpness of the lines in $NdBr_3$ could be reflected in an even smaller ratio for $\frac{1}{2}\{s_x(Z_1)+s_y(Z_1)\}/s_z(Z_1)$, if our attributing line broadening to be the principal effects of the S_+S_- terms is correct.

Work on these crystals is being continued, and more information should be available in the near future.

TABLE III. Evaluation of $\mathcal{J}_{ij}(z)=2\Delta E$ (nondipolar) $\times\left\{s_{\parallel i}s_{\parallel j}\frac{g_i^{-1}}{g_i}\frac{g_j^{-1}}{g_j}\right\}^{-1}$ (in units of cm^{-1}).

Level	L-S coupling term	$(g-1)/g$	$\mathcal{J}$(n-n)	$\mathcal{J}$(n-n-n)
		$NdCl_3$		
Z_1	$^4I_{9/2}$	−0.375	0.60	
B_2	$^4F_{9/2}$	0.250	0.32	
B_4	$^4F_{9/2}$	0.250	−0.50	
G_1	$^4G_{9/2}$[a]	0.147	0.07	
I_2	$^2D_{5/2}$	0.166	0.54	
K_1	$\frac{1}{2}^2D_{3/2}+\frac{1}{2}^2P_{3/2}$	0.065	6.32	
		$NdBr_3$		
Z_1	$^4I_{9/2}$	−0.375	1.19	−0.21
C_3	$^2H_{11/2}$	0.083	0.24	−0.15
I_1	$^2P_{1/2}$	−0.500	−0.50	0.00

[a] Poor assignment.

[8] J. S. Marsh, Phys. Letters **20**, 335 (1966).

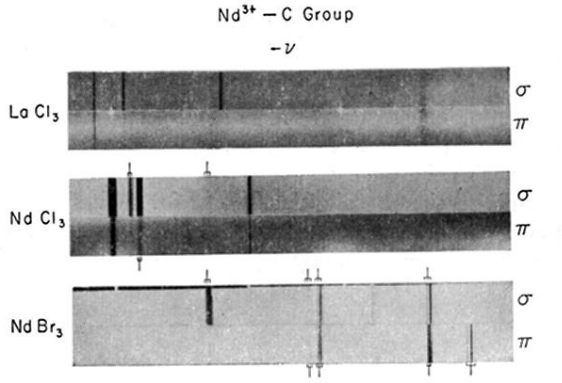

FIG. 1. *C* absorption group of Nd^{3+} ion in $LaCl_3$, $NdCl_3$, and $NdBr_3$. Region shown is 6260–6335 Å (180 cm^{-1}).

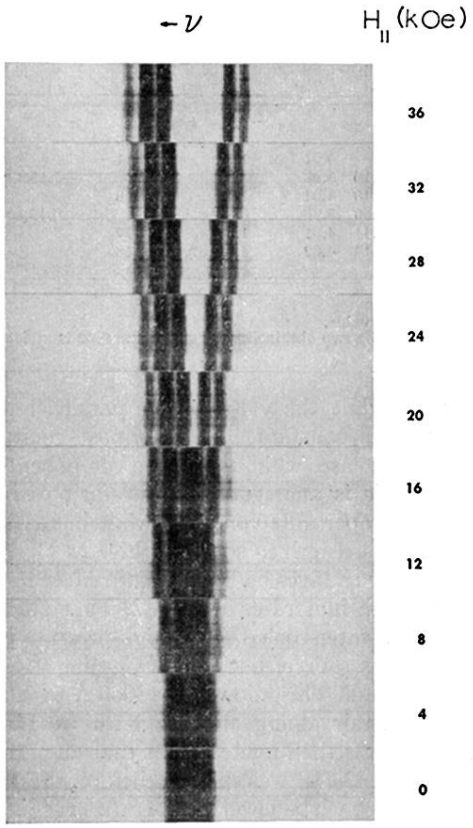

FIG. 2. Parallel Zeeman splitting of $I_1(\pi)$ in $NdBr_3$. Bath temperature is 1.5°K. Region shown is centered at $\lambda_{vac}=4241$ Å and is 5 Å (30 cm^{-1}) wide.